SUPPLEMENTAL MATERIAL

Supplemental Figure S1: Cryo-EM analysis of the Dark apoptosome.

Supplemental Figure S2: Model quality and tilt-pair validation of the correctness of the map.

Supplemental Figure S3: ATP coordination in the Dark apoptosome.

Supplemental Figure S4: Intra- and inter-protomer interactions in the Dark apoptosome.

Supplemental Figure S5: Auto-catalytically activated Dronc caspase domain is dissociated from the Dark apoptosome and remains proteolytically active.

Supplemental Figure S6: Cryo-EM analysis of the multimeric complex between Dark and Dronc-CARD.

Supplemental Figure S7: The CARD-CARD interaction between Dark and Dronc is essential for the assembly of the multimeric complex between Dark and Dronc.

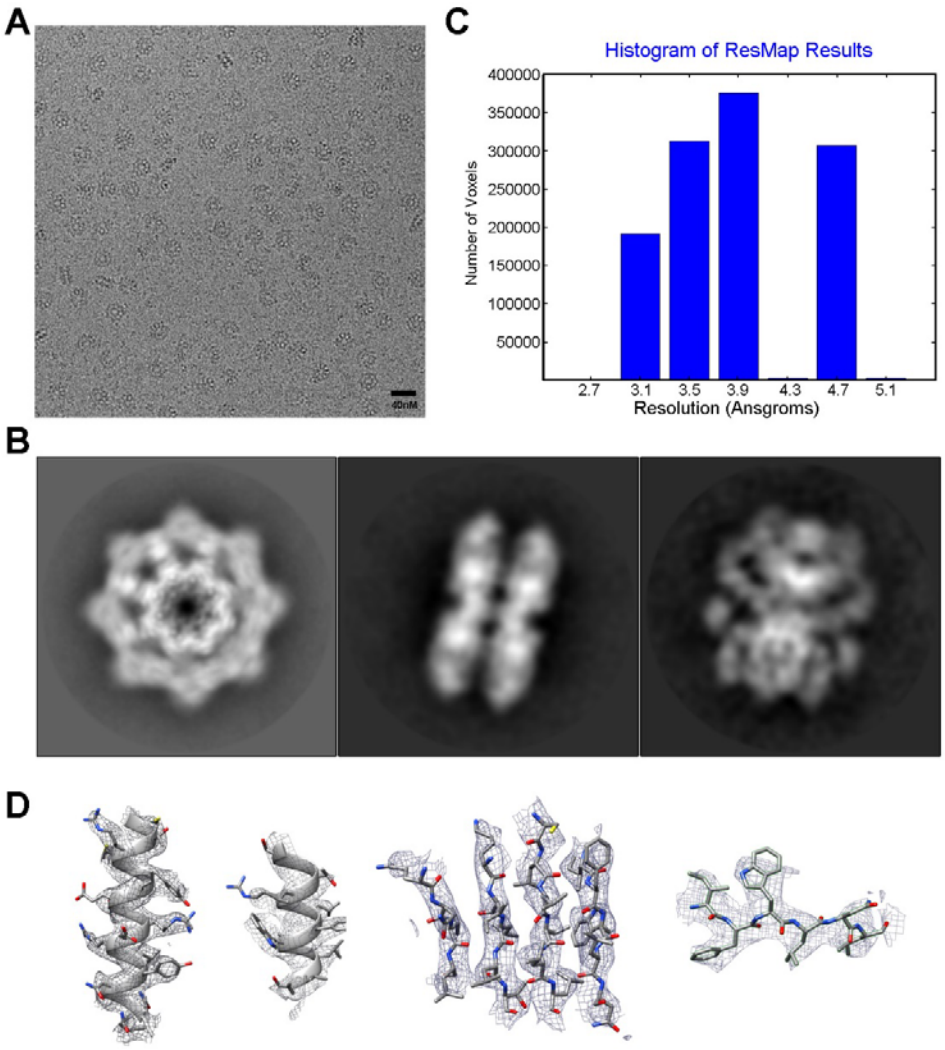

Supplemental Figure S1. Cryo-EM analysis of the Dark apoptosome. (A) Analysis of the Dark apoptosome by cryo-electron microscopy (cryo-EM). A representative electron micrograph (scale bar, 40 nm) is shown. (B) Three representative 2D classification averages of the Dark apoptosome. (C) The cryo-EM structure has an average resolution of 4.0 Å. (D) Representative EM densities are shown for select regions of the Dark apoptosome.

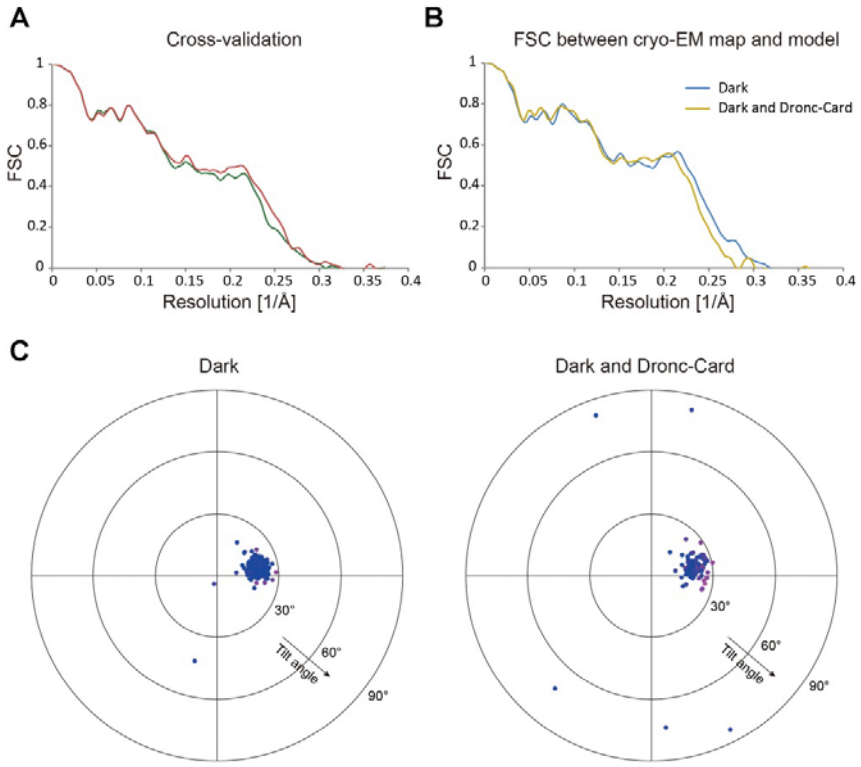

Supplemental Figure S2. Model quality and tilt-pair validation of the correctness of the map. (A) FSC curves for the Dark apoptosome. The red line represents the FSC curve between the model refined from only half of the particles and the reconstruction from that same half (FSC_{work}), whereas the green line is between the same model and the reconstruction from the other half of the particles (FSC_{test}). (B) FSC curves between the final refined atomic model and the reconstruction from all particles. (C) Particles of the Dark apoptosome and the multimeric complex between Dark and Dronc-CARD were each imaged twice at 0° and 20° tilt angles. The position of each dot represents the direction and the amount of tilting for a particle pair in polar coordinates. Blue dots correspond to in-plane tilt transformations; red dots correspond to out-of-plane tilt transformations. Most of the blue dots cluster at a tilt angle of approximately 20°, which validates the structure.

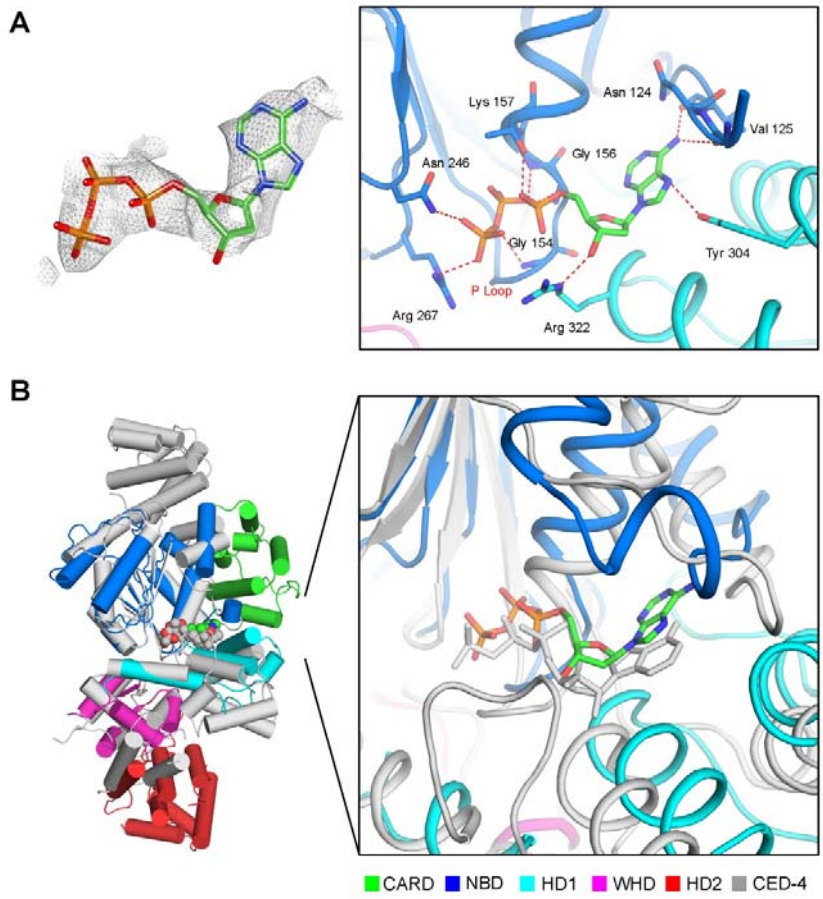

Supplemental Figure S3. ATP coordination in the Dark apoptosome. (A) dATP is surrounded by a number of polar amino acids. These residues are conserved between Dark and Apaf-1. The left panel shows the EM density of dATP, whereas the right panel displays potential H-bonds between dATP and surrounding amino acids. (B) The ATP-binding mode in Dark is reminiscent of that in CED-4. The left panel shows superposition of Dark and CED-4, with dATP/ATP shown in spheres. The middle and right panels show two perpendicular close-up views of the superposition at the dATP/ATP-binding sites.

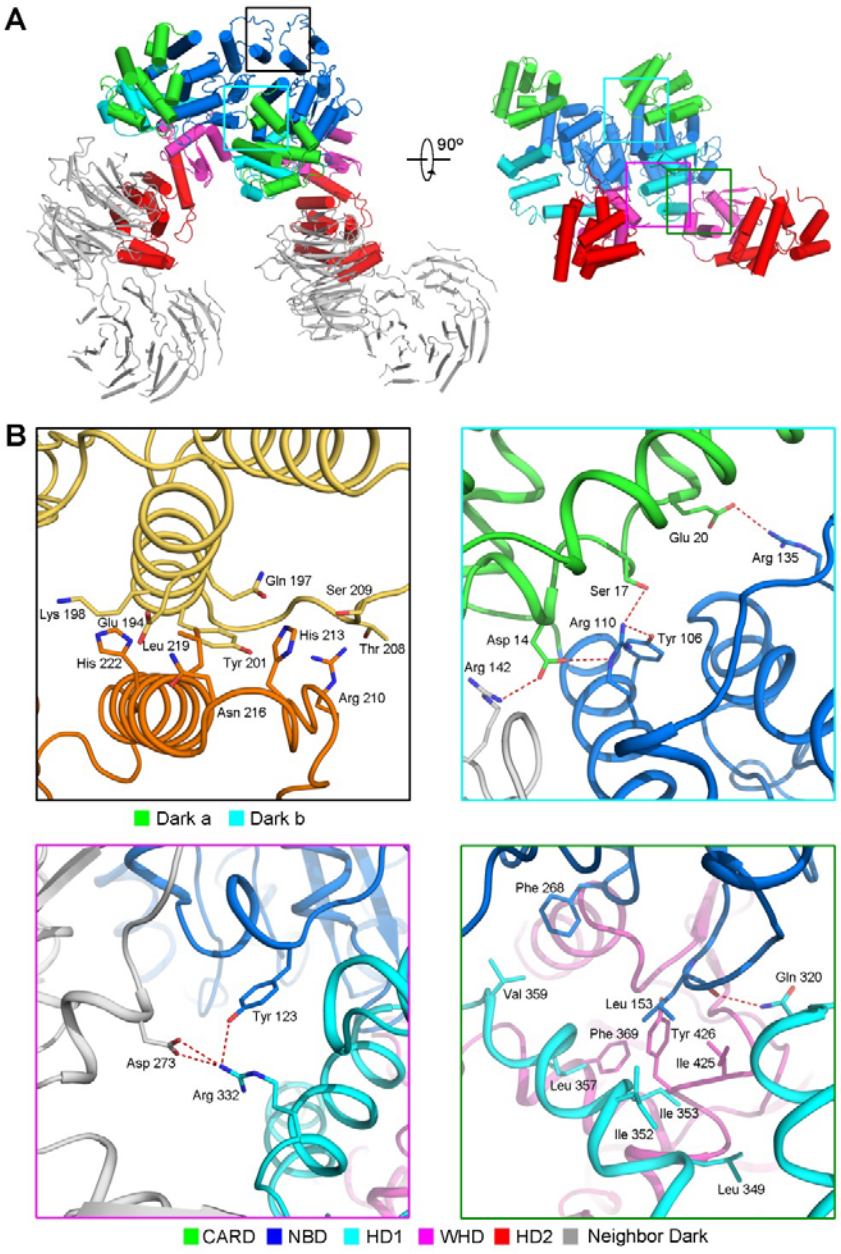

Supplemental Figure S4. Intra- and inter-protomer interactions in the Dark apoptosome. (A) Two perpendicular views of the interactions between two adjacent Dark protomers. (B) Four close-up views of the intra- and inter-protomer interactions. From left to right: interface between two neighbouring NBDs; interface among CARD and NBD within the same protomer and NBD from an adjacent protomer; interface among NBD and HD1 within the same protomer and NBD from an adjacent protomer; interface among NBD, HD1, and WHD from the same protomer.

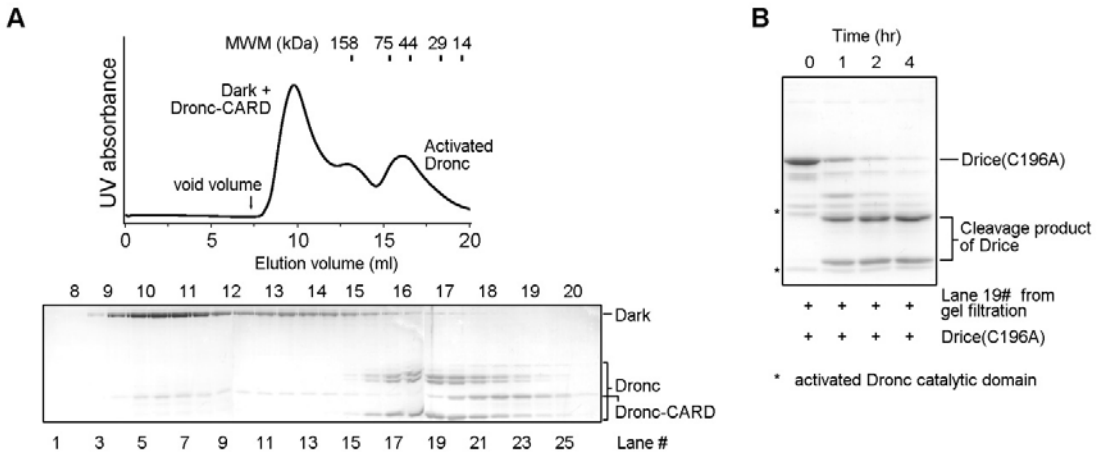

Supplemental Figure S5. Auto-catalytically activated Dronc caspase domain is dissociated from the Dark apoptosome and remains proteolytically active. (A) The fully processed caspase domain of Dronc is dissociated from the Dark apoptosome. Shown here are a gel filtration chromatogram (upper panel) and an SDS-PAGE gel stained by Coomassie blue (lower panel). (B) The fully processed caspase domain of Dronc exhibits robust protease activity towards its physiological substrate. Fraction 19 from gel filtration was examined for protease activity using Drice (residues 1-339, C196A) as the substrate. Shown here is an SDS-PAGE gel stained by Coomassie blue.

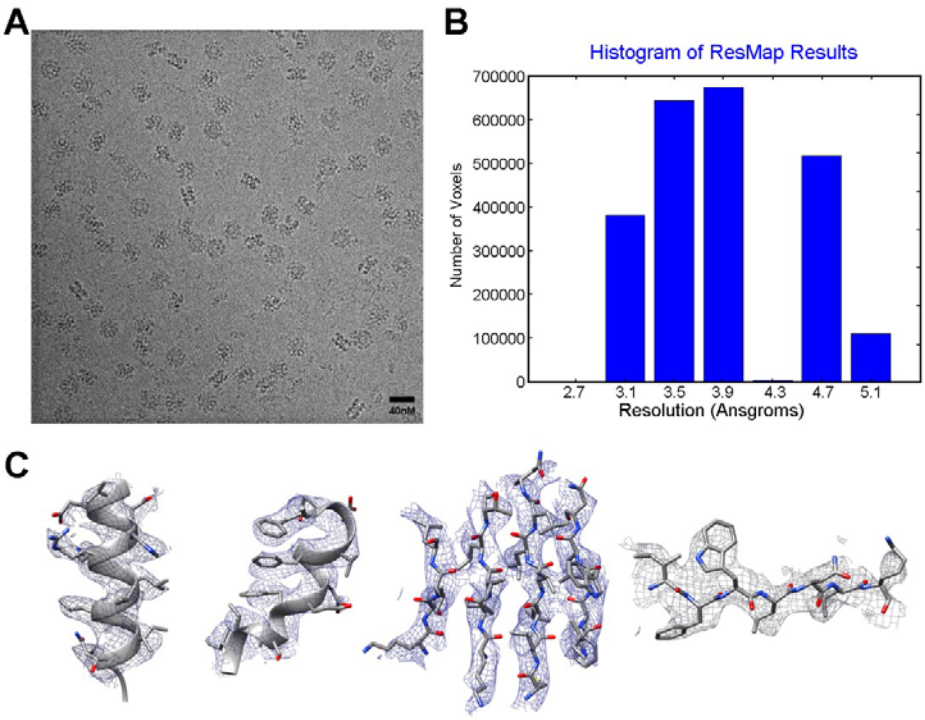

Supplemental Figure S6. Cryo-EM analysis of the multimeric complex between Dark and Dronc-CARD. (A) A representative electron micrograph (scale bar, 40 nm) of the multimeric complex between Dark and Dronc-CARD. (B) The cryo-EM structure has an average resolution of 4.1 Å. (C)Representative EM densities are shown for select regions of the multimeric complex between Dark and Dronc-CARD.

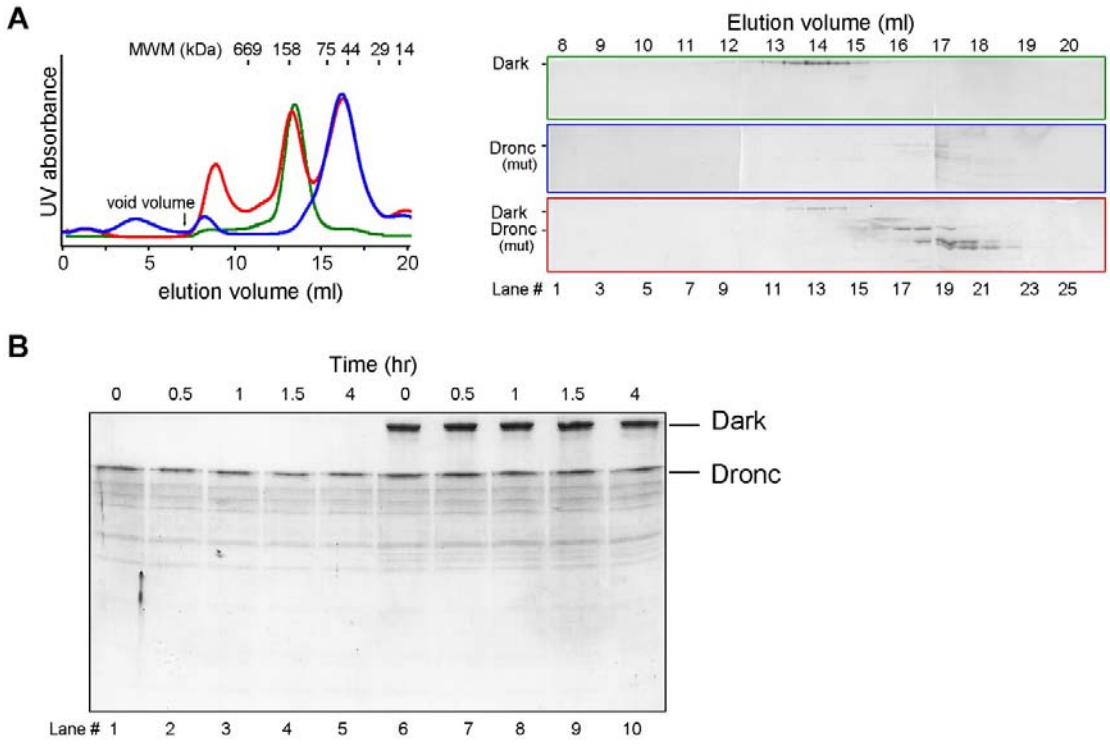

Supplemental Figure S7. The CARD-CARD interaction between Dark and Dronc is essential for the assembly of the multimeric complex between Dark and Dronc. (A) The Dronc zymogen variant (residues 1-450, C318A, Q81A/R82A) and the WT Dark failed to assemble into a multimeric complex as judged by gel filtration. Shown here are gel filtration chromatograms (left panel) and SDS-PAGE gels stained by Coomassie blue (right panel). (B) The Dronc zymogen (residues 1-450, Q81A/R82A) cannot be activated by Dark. There was no detectable processing of the Dronc zymogen upon incubation with Dark.